
Myopic Bayesian Decision Theory for Batch Active Learning with Partial Batch Label Sampling

Kangping Hu

Department of Computer Science
Georgia Institute of Technology
Atlanta, GA 30332
kangping.hu@gatech.edu

Stephen Mussmann

Department of Computer Science
Georgia Institute of Technology
Atlanta, GA 30332
mussmann@gatech.edu

Abstract

Over the past couple of decades, many active learning acquisition functions have been proposed, leaving practitioners with an unclear choice of which to use. Bayesian Decision Theory (BDT) offers a universal principle to guide decision-making. In this work, we derive BDT for (Bayesian) active learning in the myopic framework, where we imagine we only have one more point to label. This derivation leads to effective algorithms such as Expected Error Reduction (EER), Expected Predictive Information Gain (EPIG), and other algorithms that appear in the literature. A key challenge of such methods is the difficult scaling to large batch sizes, leading to either computational challenges (BatchBALD) or dramatic performance drops (top- B selection). Here, using a particular formulation of the decision process, we derive Partial Batch Label Sampling (ParBaLS) for the EPIG algorithm. We show experimentally for several datasets that ParBaLS EPIG gives superior performance for a fixed budget and Bayesian Logistic Regression on Neural Embeddings. Our code is available at <https://github.com/ADDAFT-ML/ParBaLS>.

1 Introduction

Active Learning (AL) aims to select the most informative data to label, given abundant unlabeled data but a limited labeling budget. AL approaches include heuristic-based methods [Lewis, 1995, Scheffer et al., 2001, Wang and Shang, 2014, Sener and Savarese, 2018, Ash et al., 2019, Zhang et al., 2022] and probabilistic methods [Houlsby et al., 2011, Gal et al., 2017, Kirsch et al., 2019, Ash et al., 2021, Kirsch et al., 2021, Mussmann et al., 2022, Smith et al., 2023, Huseljic et al., 2024]. From a practical point of view, most existing active learning algorithms lack explainability of when and why they work or not, making it hard for practitioners to decide which algorithm to use.

To address the issue in a theoretical and practical way, we formulate active learning based on the core principle of Bayesian Decision Theory: choose the action (point to label) that minimizes the expected cost (the test loss). A key obstacle is the intractability of planning, which we sidestep via the common myopic perspective, optimizing the test loss after one more label, rather than the entire labeling budget. From this Myopic Bayesian Decision Theory principle, we can derive expected error reduction methods Roy and McCallum [2001], Mussmann et al. [2022] and predictive entropy methods [MacKay, 1992, Smith et al., 2023].

Even with the myopic assumption, Bayesian Decision Theory encounters batching as an obstacle, a key challenge that is addressed in this work. In modern machine learning, data is typically labeled in batches rather than querying labels one-at-a-time. A common technique is to select the batch as the B samples with the highest scores, but this often leads to redundancy in selection, where similar samples with high scores are selected together. Although Kirsch et al. [2019] takes the batching issue into consideration, it requires computation that can be exponential in the batch size, making it

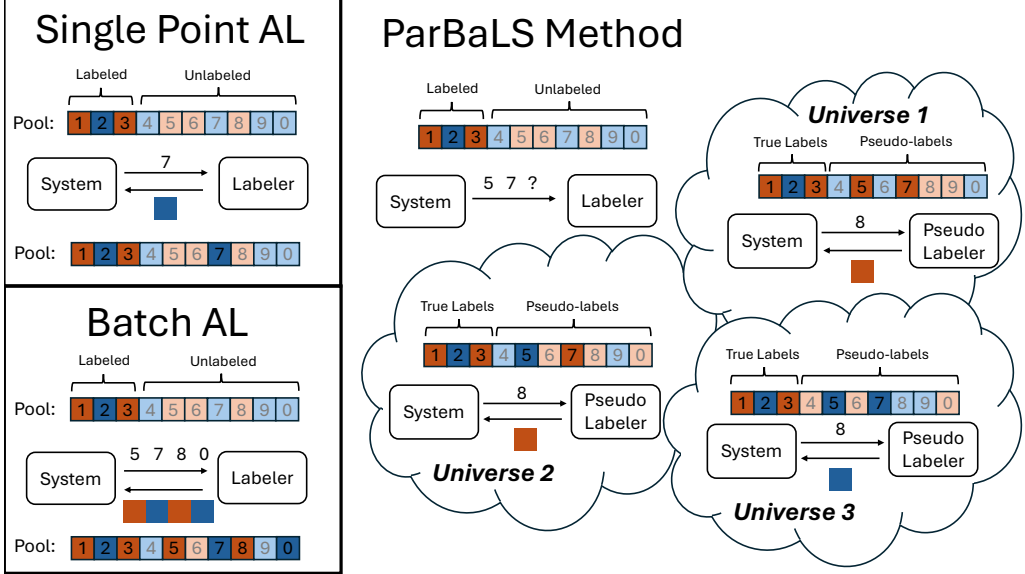


Figure 1: An illustration of the proposed method, ParBaLS. Each square denotes a datapoint: the number is the index, and the color represents the label. A dark color means the sample is labeled (by the labeler or the pseudo-labeler). After the AL system selects the sample(s) for labeling, it sends their indices (e.g. {7} for Single Point AL or {5, 7, 8, 0} for Batch AL) to the labeler, who returns the true labels of them (e.g. {blue} for Single Point AL or {red, blue, red, blue} for Batch AL). In ParBaLS, we focus on Batch AL and reduce it to Single Point AL. In the figure, we have already committed to a partial batch of {5, 7}. While we don't know the true labels, we can run single point AL in alternative universes (Universe 1, 2, and 3), where we use Monte Carlo Sampling on the posterior model parameters for pseudo-labels. Within each universe, we train a model on {1, 2, 3, 5, 7}. We can then average the active learning acquisition scores across universes to, for example, choose 8 as the next point to label. 8 is added to the partial batch, and each universe's model is updated with the universe's pseudo-label for 8. This process continues until the partial batch is complete (with B datapoints), and the AL system will send the indices of the selected batch to the labeler, as shown in Batch AL.

infeasible for large batch sizes. Kirsch et al. [2023] lowers the computational cost for batching by adding Gumbel noise to the scores for selection, but our empirical results show that they are not as effective without hyperparameter tuning. With this limitation, it has often been found [Zhang et al., 2024, Werner et al., 2024] that simpler heuristic-based algorithms like uncertainty sampling [Lewis, 1995] work equally or better than principled probabilistic algorithms.

In this paper, we present a batching approach, Partial Batch Label Sampling (ParBaLS), derived from the Myopic Bayesian Decision Theory principle. In particular, our method incrementally builds a partial batch one-at-a-time using sampled pseudo-labels to update the model. We show experimentally that ParBaLS with the EPIG criterion (equivalent to EER using the negative log likelihood loss [Mussmann et al., 2022]) has uniformly good performance across 24 different settings including tabular, text, and image datasets, with different budget and label-imbalanced settings.

Our main contributions are as follows:

- We unify several types of algorithms as derivations of the Myopic Bayesian Decision Theory (MBDT) principle, providing an intuitive and principled explanation for their performance.
- We introduce Partial Batch Label Sampling (ParBaLS) as a solution for the challenge of batching in active learning.
- We reinforce our theoretical findings by conducting experiments with Bayesian Logistic Regression on tabular datasets and image datasets with neural embeddings.

2 Setting

2.1 Batch Active Learning for Classification

Suppose we have an input domain \mathcal{X} , output domain \mathcal{Y} , and an unlabeled pool dataset $D \subset \mathcal{X}$ with an associated but hidden label $y \in \mathcal{Y}$. Thus we have a limited budget to label a subset L of D for training. The goal of Active Learning (AL) is to iteratively select T batches, $S \subset D$, of size $|S| = B$ for labeling, so that after training on the labeled set, the test loss is low.

We assume a Bayesian framework where we have a prior distribution over parameters w and a probabilistic model of $Y_x|w$, where Y_x is a random variable for the label corresponding to a datapoint x . Similarly, Y_S is a random variable for the labels corresponding to the data subset S . Our goal is to produce a predicted probability vector $p \in \Delta_{\mathcal{Y}}$ (in the probability simplex) for points drawn from a test distribution and incur low expected loss $\ell(y, p)$. For this work, we use the negative log likelihood loss $\ell(y, p) = -\ln p[y]$, where $p[y]$ is the entry of p corresponding to $y \in \mathcal{Y}$.

We assume a training procedure which, given a labeled dataset L , computes a model M_L that predicts a probability distribution over any unlabeled datapoints. We outline the high-level structure of Active Learning in Algorithm 2 and Figure 2. We also assume access to an *unlabeled* validation set $V \subset \mathcal{X}$ that is drawn from the test distribution.

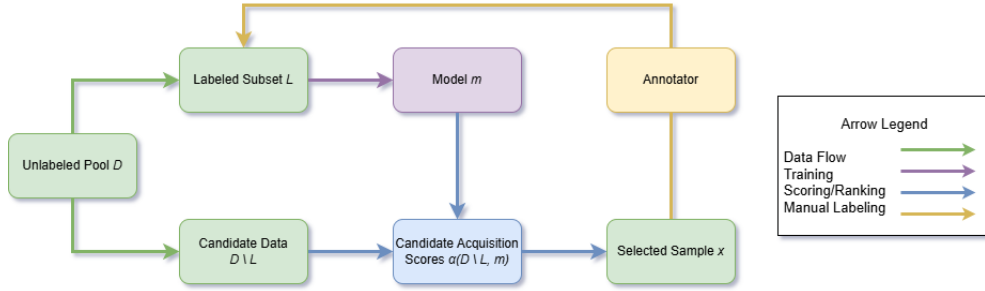


Figure 2: An illustrative diagram for Active Learning.

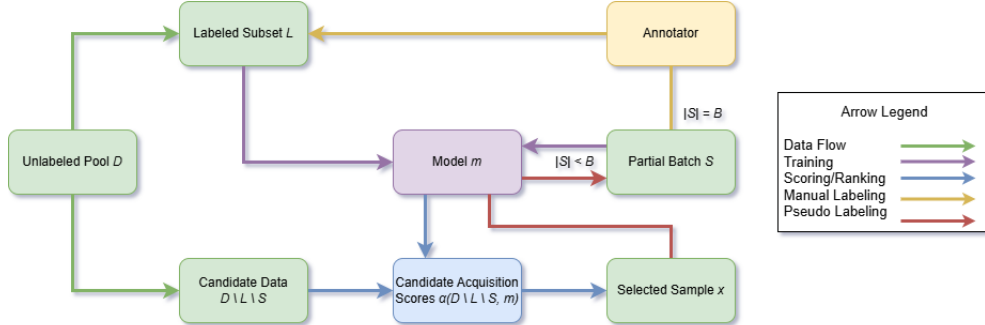


Figure 3: An illustrative diagram for ParBaLS.

2.2 (Bayesian) Logistic Regression

If $\mathcal{X} = \mathbb{R}^d$ and there are c classes, a logistic regression predictor is defined by weights $W \in \mathbb{R}^{c \times d}$ and biases $b \in \mathbb{R}^c$. Under this model, for an input x and class i , the estimated probability is $\exp(W_i x + b_i) / \sum_j \exp(W_j x + b_j)$. Given a labeled set L , we can fit W and b via maximum likelihood estimation, or equivalently, minimizing the logistic loss.

Instead of having fixed parameters after training for inference, Bayesian Logistic Regression uses a Gaussian prior for the parameters and conditions on the training data to define a posterior distribution over the parameters. For a new datapoint, we predict the expected model prediction, where the models are drawn from the posterior. Given the complexity of continuous integrals, we use a Monte

Carlo estimate for Bayesian Model Averaging. Let k be the number of posterior parameter samples drawn from the Bayesian model. In our work, we sample from the posterior using the NUTS sampler [Hoffman et al., 2014], the default sampler in PyMC [Abril-Pla et al., 2023].

Although deep neural networks pose a computational issue for full fine-tuning, especially during Active Learning iterations, we can freeze all the weights except the last layer as a proxy model to select batches of data based on their embeddings from fixed encoders, which has been shown to be experimentally effective [Zhang et al., 2024]. This is known as Linear Probing, which is equivalent to Logistic Regression, as we consider the fixed embeddings as the features. We can also use Bayesian Logistic Regression as the last layer, empowering superior uncertainty quantification for AL as well as improved model performance. Using linear probing, we benefit from the growing availability of effective embedding models, achieving both efficiency and performance. Other Bayesian approaches to neural networks exhibit non-Bayesian properties Pituk et al. [2025], which supports our choice of BLR on neural embeddings as a more statistically grounded modelling choice.

2.3 Bayesian Decision Theory

Bayesian Decision Theory provides a formal framework for making optimal decisions under uncertainty. It is grounded in the principles of probability theory and utility theory, combining prior beliefs with observed data to guide rational decision-making. At its core, the theory assumes that all uncertainty can be quantified probabilistically, and that decisions should be made to minimize expected cost.

The core idea is that we have a Bayesian Posterior P over hidden world states Θ , a set of actions A , and a cost function $C : \Theta \times A \rightarrow \mathbb{R}$. Then, the BDT principle is to select the action $a \in A$ that minimizes $\mathbb{E}_{\theta \sim P}[C(\theta, a)]$.

3 Myopic Bayesian Decision Theory (MBDT)

For active learning, we have a sequence of actions instead of a single action: first, we sequentially choose batches of data points to label, then finally, we make predictions on test or validation points.

Due to the complexity of multi-turn optimization, following the vast majority of active learning work, we focus on myopic decisions. Assume we have a labeled set L and we want to choose one more data point \hat{x} from D (and will receive label \hat{y}), then we will make probabilistic predictions $P \in \Delta_{\mathcal{Y}}^{|V|}$ on validation points $V \subset \mathcal{X}$. With $\vec{y} \in \mathcal{Y}^{|V|}$ and y_j being its j -th entry, the next point to label is:

$$\arg \min_{\hat{x} \in D} \mathbb{E}_{\hat{y} \sim Y_{\hat{x}} | L} \left[\min_{P \in \Delta_{\mathcal{Y}}^{|V|}} \mathbb{E}_{\vec{y} \sim Y_V | Y_{\hat{x}} = \hat{y}, L} \left[\sum_{j=1}^{|V|} \ell(y_j, P_j) \right] \right] \quad (1)$$

For the negative log loss $\ell(y, p) = -\ln p[y]$, the optimal P is simply the posterior distribution (see details for this result and the following derivation in Appendix A) and thus the expected loss reduces to the entropy:

$$\arg \min_{\hat{x} \in D} \mathbb{E}_{\hat{y} \sim Y_{\hat{x}} | L} \left[\sum_{x \in V} H(Y_x | Y_{\hat{x}} = \hat{y}, L) \right] \quad (2)$$

Using the fact that $H(Y|X) = H(Y) - I(X; Y)$ for random variables X and Y , and that $H(Y_x | L)$ for $x \in V$ doesn't depend on \hat{x} , we can equivalently choose the point,

$$\arg \max_{\hat{x} \in D} \sum_{x \in V} I(Y_x; Y_{\hat{x}} | L) \quad (3)$$

This is the same form as EPIG [Kirsch et al., 2021, Smith et al., 2023] (motivated by predictive mutual information), EER (motivated by reducing expected error, see derivation in Mussmann et al. [2022]), and a method from one of the first active learning papers [MacKay, 1992].

3.1 Batching

In the above derivation, we assumed that we only choose one new point to label, \hat{x} . To extend this to the batch setting, we categorize existing strategies into three groups:

Top- B Compute the score for each point in the pool, then take the B points with the highest scores. Unfortunately, this method ignores the dependencies between batch labels and can be very sub-optimal. For example, this strategy may select a batch composed of a single datapoint duplicated many times. See Kirsch et al. [2019] for more intuition and examples.

Heuristic Diversity Heuristically add randomness or diversity to the batch. For example, Kirsch et al. [2023] randomly perturbs the scores and takes the top- B , and Wei et al. [2015] uses submodular maximization to pick a diverse subset of the top-scoring points. Such methods unfortunately require tuning dataset-specific hyperparameters, which are infeasible to tune for active learning, where we collect data once. Though Kirsch et al. [2023] finds that a default hyperparameter ($\beta = 1$) works well uniformly, we arrive at a different conclusion in our experiments. Intuitively, the level of randomness depends on the level of statistical dependency between high-scoring points, which is dataset-specific.

Greedy Batch Acquisition We can replace optimizing $\hat{x} \in D$ with optimizing a batch of points $\hat{X} \subset D$ with $|\hat{X}| = B$. BAIT [Ash et al., 2021] and BatchBALD [Kirsch et al., 2019] optimize \hat{X} via greedy subset selection. While this strategy is relatively computationally efficient for (non-Bayesian) BAIT, especially with efficient algorithmic modifications [Huseljic et al., 2024], it is not for (Bayesian) BatchBALD. A major challenge is that for a batch \hat{X} of size B , for fixed values of the batch labels \hat{Y} , the required number of Bayesian posterior parameter samples (k in Kirsch et al. [2019]) to “cover” \hat{Y} grows exponentially in the batch size.

3.2 ParBaLS

Here we introduce an alternative approach, similar to some pseudo-labeling strategies outside of active learning [Jiang et al., 2017]. Here, in addition to the labeled set L , we have a set S of unlabeled points that we’ve committed to labeling but haven’t seen the labels (a partial batch). For this state, the next (myopically) optimal point according to Bayesian Decision Theory is,

$$\arg \min_{\hat{x} \in D} \mathbb{E}_{\hat{y}, y_S \sim Y_{\hat{x}}, Y_S | L} \left[\sum_{x \in V} H(Y_x | Y_{\hat{x}} = \hat{y}, Y_S = y_S, L) \right] \quad (4)$$

Similar to the earlier one-at-a-time (i.e., $B = 1$) case, we can subtract $H(Y_x | Y_S, L)$, which doesn’t depend on \hat{x} , and equivalently choose,

$$\arg \max_{\hat{x} \in D} \mathbb{E}_{y_S \sim Y_S | L} \left[\sum_{x \in V} I(Y_x; Y_{\hat{x}} | Y_S = y_S, L) \right] \quad (5)$$

In order to compute or estimate the expectation, we would need to sum over y_S , which has size exponential in the batch size. We can use a Monte Carlo estimate by first sampling m versions of $y^{(i)} \sim Y_D | L$ and selecting,

$$\arg \max_{\hat{x} \in D} \frac{1}{m} \sum_{i=1}^m \sum_{x \in V} I(Y_x; Y_{\hat{x}} | Y_S = y_S^{(i)}, L) \quad (6)$$

A key advantage is that we can incrementally train m parallel models on $y_S^{(i)}$ to avoid the issue of requiring a number of parameter posterior samples that is exponential in the batch size. Critically, the variance of the Monte Carlo estimate decays as $\mathcal{O}(1/\sqrt{m})$ and does not depend on the batch size. For Bayesian Logistic Regression with k posterior parameters, we can sample $m \leq k$ possibilities of the labels of $D \setminus L$, each called $y^{(i)} \sim Y_{D \setminus L} | L$. For each selection, we compute the acquisition score according to Equation 6. After selecting each sample \hat{x} in a batch, we assign m versions of pseudo labels $y_{\hat{x}}^{(i)}$ to it. With each version i , we add $(\hat{x}, y_{\hat{x}}^{(i)})$ to the training set of M_i and update

Method	Time Complexity	Space Complexity
Top- B	$O(N \cdot k \cdot C)$	$O(k \cdot d \cdot C)$
BatchBALD	$O(N \cdot k \cdot C^B)$	$O(N \cdot k \cdot C)$
ParBaLS (Ours)	$O(B \cdot N \cdot m \cdot k \cdot C)$	$O(m \cdot k \cdot d \cdot C)$

Table 1: Comparison of Time and Space Complexity. N : pool size, B : batch size, k : number of posterior parameter samples, m : number of universes for ParBaLS, C : number of classes, d : embedding dimension.

Algorithm 1 ParBaLS EPIG

Input: unlabeled pool D ;
 unlabeled validation set V ;
 currently labeled subset L ;
 model training procedure M ;
 budget B

Output: Batch S for labeling

- 1: $S \leftarrow \emptyset$
- 2: Train Bayesian model $M_L = M(L)$
- 3: **for** $i \leftarrow 1$ **to** m **do**
- 4: Using M_L , sample $y^{(i)} \sim Y_{D \setminus L} | L$
- 5: Initialize $M_i = M_L$
- 6: **end for**
- 7: **for** $j \leftarrow 1$ **to** B **do**
- 8: Compute \hat{x} as

$$\arg \max_{\hat{x} \in D} \sum_{i=1}^m \sum_{x \in V} I(Y_x; Y_{\hat{x}} | Y_S = y_S^{(i)}, L)$$
- 9: $S \leftarrow S \cup \{\hat{x}\}$
- 10: $D \leftarrow D \setminus \{\hat{x}\}$
- 11: **for** $i \leftarrow 1$ **to** m **do**
- 12: Update M_i with datapoint $(\hat{x}, y_{\hat{x}}^{(i)})$ (i.e. $M_i = M(L \cup \{(x, y_x^{(i)}) : x \in S\})$)
- 13: **end for**
- 14: **end for**
- 15: **return** S

it with both real labels from L and pseudo labels from the partial batch S . For the next sample to select, we use the joint score from m semi-pseudo models to take the overall best one. We outline a high-level algorithm for ParBaLS EPIG in Algorithm 1. We also provide an illustrative diagram in Figure 3 with an example in Figure 1.

Treating the train time as constant, we provide a comparison of time and space complexity between Top- B , BatchBALD Kirsch et al. [2019], and our ParBaLS in Table 1.

ParBaLS-MAP While the main version of ParBaLS requires sampling m versions of $y^{(i)}$, another variant we test experimentally involves using just one version of labels $y^{(1)}$ comprised of the Maximum A Posteriori (MAP) labels for each unlabeled point: $y_x^{(i)} = \arg \max_{y \in \mathcal{Y}} \Pr(Y_x = y | L)$.

Dataset	Encoder	Before PCA	After PCA
CIFAR-10	DINOv2-ViT-S/14	384	348
CIFAR-100	DINOv2-ViT-S/14	384	353
iWildCam	CLIP-ViT-B/32	512	305
fMoW	CLIP-ViT-B/32	512	342
AG News	bert_base_uncased	768	210

Table 2: Comparison between the embedding dimensions before and after 99% PCA for each dataset with its encoder.

Datasets Algorithm	Airline Passenger Satisfaction	Credit Card Fraud	One-vs-all				Subpopulation-shifted					
			CIFAR-10	CIFAR-100	iWildCam	fMoW	AG News	CIFAR-10	CIFAR-100	iWildCam	fMoW	AG News
BALD	86.91 \pm 1.38	93.25\pm0.27	87.31 \pm 1.39	95.38\pm1.06	74.05 \pm 1.51	89.82 \pm 3.31	70.47 \pm 3.05	72.08 \pm 1.89	37.80 \pm 16.33	70.87 \pm 1.96	23.56 \pm 3.67	72.53 \pm 1.89
PowerBALD	88.54 \pm 0.64	93.37\pm0.23	88.02 \pm 0.72	89.51 \pm 1.23	84.21 \pm 2.01	91.25 \pm 1.76	84.04 \pm 0.75	78.76 \pm 4.05	62.20 \pm 12.19	77.10 \pm 2.78	19.59 \pm 8.38	75.53 \pm 1.48
SoftmaxBALD	86.92 \pm 0.69	92.74 \pm 0.37	87.88 \pm 1.54	90.16 \pm 0.46	84.42 \pm 2.93	90.93 \pm 1.40	83.77 \pm 1.23	80.14 \pm 3.82	62.20 \pm 11.60	78.82 \pm 2.27	23.84 \pm 8.33	75.72 \pm 0.85
SoftRankBALD	88.14 \pm 0.48	93.37\pm0.19	90.50 \pm 1.48	95.87\pm0.27	80.48 \pm 1.11	93.28 \pm 3.40	84.76 \pm 1.09	76.86 \pm 2.35	54.40 \pm 16.69	77.05 \pm 2.82	13.84 \pm 8.13	76.40 \pm 2.04
EPiG	88.81\pm0.48	93.25\pm0.38	92.26 \pm 1.02	94.54 \pm 0.88	82.32 \pm 1.53	96.02\pm1.66	87.13\pm0.60	93.74 \pm 0.74	88.20\pm2.04	78.95 \pm 4.57	38.36\pm2.08	84.40 \pm 1.79
PowerEPiG	87.41 \pm 0.86	92.96 \pm 0.41	87.54 \pm 1.02	89.24 \pm 1.01	84.93 \pm 0.82	90.21 \pm 1.80	83.45 \pm 0.98	79.88 \pm 3.30	57.00 \pm 20.75	74.28 \pm 3.78	19.45 \pm 5.17	76.13 \pm 1.78
SoftmaxEPiG	87.94 \pm 0.58	93.00\pm0.48	88.80 \pm 0.48	90.51 \pm 0.62	84.88 \pm 0.61	91.24 \pm 1.51	84.77 \pm 0.80	86.80 \pm 1.26	70.60 \pm 4.67	77.10 \pm 4.87	17.53 \pm 5.19	78.51 \pm 1.95
SoftRankEPiG	88.34 \pm 0.28	93.42\pm0.23	90.74 \pm 0.53	93.04 \pm 0.69	85.33\pm1.71	95.30 \pm 1.40	86.11 \pm 0.88	92.54 \pm 0.36	86.60\pm2.73	78.51\pm6.05	23.97 \pm 6.31	83.97 \pm 1.51
ParBalS-MAP EPiG	89.34\pm0.46	93.45\pm0.29	93.40\pm1.19	95.82\pm0.98	87.60\pm1.62	97.24\pm1.10	86.71 \pm 1.00	94.74\pm1.04	89.00\pm1.90	84.05\pm3.31	27.40 \pm 7.68	86.26\pm0.69
ParBalS EPiG	89.35\pm0.60	93.45\pm0.22	94.90 \pm 0.54	96.03 \pm 0.67	85.97 \pm 1.32	98.03 \pm 0.58	87.73 \pm 0.67	95.30\pm0.30	88.00\pm3.29	82.12\pm3.19	27.95 \pm 12.03	86.21\pm0.92

Table 3: Final test accuracy of Bayesian-based AL algorithms with Bayesian Logistic Regression, where each of the 10 iterations has a labeling budget of 20 samples, except for the first iteration that starts with 100 samples.

Datasets Algorithm	Airline Passenger Satisfaction	Credit Card Fraud	One-vs-all				Subpopulation-shifted					
			CIFAR-10	CIFAR-100	iWildCam	fMoW	AG News	CIFAR-10	CIFAR-100	iWildCam	fMoW	AG News
BALD	88.94\pm0.48	93.34\pm0.16	97.92 \pm 0.17	99.74\pm0.05	91.25\pm1.09	99.78\pm0.02	88.43 \pm 0.57	90.44 \pm 1.65	69.40 \pm 5.89	83.13\pm2.45	14.52 \pm 6.39	83.23 \pm 1.38
PowerBALD	88.77 \pm 0.56	93.30 \pm 0.22	97.25 \pm 0.48	99.17 \pm 0.06	91.41\pm0.93	98.81 \pm 0.30	88.06 \pm 0.39	87.74 \pm 1.63	61.60 \pm 6.38	82.56\pm3.25	16.16 \pm 6.72	83.23 \pm 0.67
SoftmaxBALD	88.32 \pm 0.65	93.25 \pm 0.19	96.84 \pm 0.76	98.85 \pm 0.22	91.20\pm1.49	98.83 \pm 0.29	88.17 \pm 0.51	87.88 \pm 1.13	63.80 \pm 6.14	81.92 \pm 2.46	16.85 \pm 7.89	82.68 \pm 1.13
SoftRankBALD	88.90\pm0.67	93.32\pm0.29	97.80 \pm 0.35	99.72\pm0.07	92.08\pm1.17	99.76\pm0.04	88.65 \pm 0.64	89.62 \pm 1.61	71.00 \pm 5.22	82.26 \pm 2.83	10.14 \pm 4.40	83.41 \pm 1.08
BatchBALD	89.08\pm0.43	93.36 \pm 0.23	98.00 \pm 0.18	99.71\pm0.07	91.83 \pm 0.76	99.79\pm0.01	88.50 \pm 0.78	90.18 \pm 0.84	63.80 \pm 4.75	83.47\pm2.38	11.92 \pm 7.33	(Too slow)
EPiG	89.28\pm0.41	93.45 \pm 0.28	98.05\pm0.34	99.60 \pm 0.08	90.43\pm1.97	99.73 \pm 0.00	89.36\pm0.49	93.96 \pm 0.60	88.00\pm1.67	84.68\pm2.69	27.95\pm11.06	85.27\pm0.44
PowerEPiG	88.30 \pm 0.78	93.24 \pm 0.36	96.62 \pm 0.31	99.76 \pm 0.21	90.26 \pm 1.81	98.24 \pm 0.82	87.97 \pm 4.42	88.58 \pm 1.95	61.20 \pm 3.76	82.00\pm3.34	19.86 \pm 11.34	83.41 \pm 0.01
SoftmaxEPiG	88.29 \pm 0.93	93.31 \pm 0.21	97.12 \pm 0.35	99.10 \pm 0.12	91.24\pm0.39	98.53 \pm 0.86	88.01 \pm 0.80	89.84 \pm 1.02	66.60 \pm 4.33	83.00\pm2.23	17.26 \pm 8.81	84.06 \pm 0.45
SoftRankEPiG	88.26 \pm 0.31	93.36 \pm 0.29	97.85 \pm 0.31	99.58 \pm 0.05	91.14\pm0.73	99.39\pm0.48	89.09\pm0.49	92.76 \pm 1.01	86.00 \pm 1.00	84.51\pm2.39	27.95\pm5.69	85.31\pm0.60
ParBalS-MAP EPiG	89.15 \pm 0.47	93.45 \pm 0.33	98.26\pm0.30	99.62 \pm 0.05	91.92\pm1.22	99.53\pm0.47	89.30\pm0.49	94.00 \pm 0.24	89.60\pm1.85	85.22\pm2.29	24.93 \pm 2.66	85.33 \pm 1.33
ParBalS EPiG	89.42\pm0.41	93.55 \pm 0.23	98.20 \pm 0.27	99.66 \pm 0.15	92.17 \pm 1.12	99.76 \pm 0.03	89.41 \pm 0.72	94.86\pm0.41	87.80 \pm 1.72	84.72\pm1.98	31.37 \pm 6.60	85.72 \pm 1.02

Table 4: Final test accuracy of Bayesian-based AL algorithms with Bayesian Logistic Regression, where each of the 10 iterations has a labeling budget of 10 samples, except for the first iteration that starts with 500 samples.

4 Experiments

4.1 Datasets

Following a recent benchmark [Zhang et al., 2024] on active learning, we conduct our experiments on both standard datasets (CIFAR-10 and CIFAR-100 [Krizhevsky et al., 2009]) and real-world datasets (iWildCam [Beery et al., 2021] and fMoW [Christie et al., 2018] from the WILDS [Koh et al., 2021] benchmark) for image classification. However, these benchmarks are mostly image datasets, where typically the label can be determined exactly from the input features. On the other hand, when there is irreducible uncertainty, heuristic-based algorithms fail to capture these aspects, while EER-based algorithms perform well. We thus also include two tabular datasets from Kaggle, Airline Passenger Satisfaction [Klein, 2020] and Credit Card Fraud [Narayanan, 2022], as well as AG News [Gulli, 2004], a classic text classification dataset, which are often overlooked by common benchmarks but can demonstrate the advantages of EER algorithms where uncertainty-based algorithms fail.

One-vs-all datasets For image and text datasets, we first explore an imbalanced scenario, where the set of labels is imbalanced but consistent between the train set and the test set. As data selection matters more in the imbalanced datasets, we convert each of the original image datasets into two classes, with one being the first original class and the other one being the rest of the original classes. We call this setting “one-vs-all”.

Subpopulation-shift datasets We additionally convert each of the image or text datasets into three classes, with the first one being the first original class, the second one being the second original class, and the third one being the rest of the original classes. While all classes appear in the pool, we are only tested on the first two classes. This realistically models ML tasks where the pool has irrelevant data that is not the target. We call this setting “subpopulation-shift” as the test set is a subpopulation of the train set.

4.2 Models

To improve the efficiency of the selection process, we fix an embedding model and conduct active learning with Bayesian Logistic Regression on the embeddings. The embedding models include the CLIP-ViT-B/32 [Radford et al., 2021] for the WILDS datasets, DINOv2-ViT-S/14 models [Oquab et al., 2024] for CIFAR-10 and CIFAR-100, and BERT [Devlin et al., 2019] for AG News, which are widely used in recent studies [Zhang et al., 2024, Huseljic et al., 2024]. To avoid numeric issues, we apply PCA to reduce the embedding space while retaining 99% of the variance. The details of the

Datasets Algorithm	Airline Passenger Satisfaction	Credit Card Fraud	One-vs-all			Subpopulation-shifted		
			CIFAR-10	CIFAR-100	iWildCam	CIFAR-10	CIFAR-100	iWildCam
Random	87.23 \pm 0.53	92.71 \pm 0.28	87.41 \pm 0.74	88.76 \pm 0.70	83.51 \pm 1.50	90.56 \pm 1.24	84.28 \pm 0.83	76.14 \pm 4.16
Confidence	89.16\pm0.32	92.91 \pm 0.38	95.28\pm0.80	98.55\pm0.26	99.98\pm1.42	99.26\pm0.36	86.54 \pm 0.80	82.80 \pm 2.01
GLISTER	87.23 \pm 1.36	93.59\pm0.23	89.04 \pm 1.59	93.38 \pm 1.19	76.64 \pm 2.69	89.63 \pm 1.80	81.88 \pm 2.76	68.60 \pm 4.46
ParBaLS-MAP EPIG	89.34\pm0.46	93.48\pm0.29	93.40 \pm 1.19	95.82 \pm 0.98	87.60 \pm 1.62	97.24 \pm 1.10	86.71 \pm 1.00	94.74\pm1.04
ParBaLS EPIG	89.35\pm0.60	93.45\pm0.22	94.90 \pm 0.54	96.03 \pm 0.67	85.97 \pm 1.32	98.03 \pm 0.58	87.73\pm0.67	95.30\pm0.30
							88.00 \pm 3.29	82.12 \pm 3.19
								27.95 \pm 12.03
								86.21 \pm 0.92

Table 5: Final test accuracy of ParBaLS and heuristics baselines with Bayesian Logistic Regression, where each of the 10 iterations has a labeling budget of 20 samples, except for the first iteration that starts with 100 samples.

encoders and dimensions before and after PCA for each dataset are shown in Table 2. For tabular datasets, we directly apply Bayesian Logistic Regression after preprocessing (apply quantile binning with 10 bins to numerical features, then apply one-hot encoding to all features). We use $k = 400$ posterior parameter samples for Bayesian Logistic Regression in all our experiments.

4.3 Active Learning Algorithms

For Bayesian active learning baselines, we evaluate EPIG [Kirsch et al., 2021, Mussmann et al., 2022, Smith et al., 2023] and BALD [Houlsby et al., 2011, Gal et al., 2017], where each of them is combined with either the standard top- B batch selection, one of the three Gumbel noise methods [Kirsch et al., 2023], or BatchBALD [Kirsch et al., 2019] for BALD. For non-Bayesian methods we include Random, Confidence [Lewis, 1995], GLISTER [Killamsetty et al., 2021] as our baselines. For fair comparison, we use the calibrated, more accurate probabilities from our Bayesian Logistic Regression model. Our proposed algorithms are EPIG with our ParBaLS-MAP and ParBaLS. We use $m = 10$ universes for ParBaLS in our main experimental results. Following Mussmann et al. [2022], we randomly subsample a subset of the candidate pool and validation set during each iteration, whose sizes are 10000 and 1000, respectively, regardless of which dataset we use. For GLISTER, we use 20% of the initial labeled set as the labeled validation set.

4.4 Experimental Details

We conduct our experiments with the NVIDIA RTX 6000 GPU on a Slurm-based cluster Yoo et al. [2003], using the LabelBench package [Zhang et al., 2024], a well-established framework to benchmark label-efficient learning, including active learning. For each setting, we conduct 5 runs with different seeds to gauge the variability of our results. We report the average performance over the 5 runs and show twice the standard error¹ with “ \pm ”. We consider a method to be within the top (bolded in our presented tables) if its mean is within the \pm of the method with the highest mean, or vice versa.

4.5 Experimental Results

We run experiments with two data budget settings. The first uses a smaller initial labeled dataset, we use $T = 10$ iterations each with an iteration budget of $B = 20$, except for the first iteration that starts with 100 randomly sampled points, as shown in Table 3 and 5. The second uses a larger initial labeled dataset, we use $T = 10$ iterations each with an iteration budget of $B = 10$, except for the first iteration that starts with 500 random samples, as shown in Table 4 and 6. BatchBALD [Kirsch et al., 2019] is too slow with the larger batch sizes, so we only include it in the second budget setting ($B = 10$ rather than $B = 20$).

For both budget settings, we first compare various Bayesian-based AL algorithms, in Table 3 and 4.

For both budget settings, the EPIG variants outperform the BALD variants with both top- B and Gumbel batching methods. Specifically, ParBaLS EPIG stays among the top for all datasets, which demonstrates the effectiveness of ParBaLS EPIG among the various Bayesian-based AL algorithms.

With ParBaLS EPIG and ParBaLS-MAP EPIG being the best among the Bayesian-based AL algorithms, we further compare them with heuristic baselines in Table 5 and 6.

We note that GLISTER requires an initial labeled validation set, which can limit its applicability in scenarios with a small initial budget. On the other hand, although Confidence performs well in

¹A Gaussian 95% confidence interval formed using $1.96 \approx 2$ standard error.

Datasets Algorithm	Airline Passenger Satisfaction	Credit Card Fraud	One-vs-all				Subpopulation-shifted					
			CIFAR-10	CIFAR-100	iWildCam	fMoW	AG News	CIFAR-10	CIFAR-100	iWildCam	fMoW	AG News
Random	98.46 \pm 0.68	93.18 \pm 0.34	96.76 \pm 0.38	98.78 \pm 0.26	91.12 \pm 0.87	98.47 \pm 0.44	87.99 \pm 0.59	87.90 \pm 1.73	77.40 \pm 2.73	81.79 \pm 3.94	19.18 \pm 0.87	82.48 \pm 1.19
Confidence	89.27\pm0.42	93.41\pm0.36	98.45\pm0.19	99.75\pm0.05	93.39\pm0.47	99.74\pm0.09	89.18\pm0.59	89.28\pm0.75	74.40\pm4.56	83.68\pm3.20	9.04\pm4.87	84.66\pm1.08
GLISTER	88.89 \pm 0.28	93.43 \pm 0.30	97.92 \pm 0.14	99.54 \pm 0.04	91.00 \pm 1.18	99.39\pm0.55	88.23 \pm 0.30	87.88 \pm 0.54	62.20 \pm 4.07	81.70 \pm 1.91	25.07\pm3.82	82.96 \pm 1.20
ParBaLS-MAP EPIG	89.15\pm0.47	93.45\pm0.33	98.26\pm0.30	99.62 \pm 0.05	91.92 \pm 1.22	99.53\pm0.47	89.30\pm0.49	94.00 \pm 0.24	89.60\pm1.85	85.22\pm2.29	24.93\pm2.66	85.33\pm1.33
ParBaLS EPIG	89.42\pm0.41	93.55\pm0.23	98.20\pm0.27	99.66\pm0.15	92.17 \pm 1.12	99.76\pm0.03	89.41\pm0.72	94.86\pm0.41	87.80\pm1.72	84.72\pm1.98	31.37\pm6.60	85.47\pm0.91

Table 6: Final test accuracy of ParBaLS and heuristics baselines with Bayesian Logistic Regression, where each of the 10 iterations has a labeling budget of 10 samples, except for the first iteration that starts with 500 samples.

Algorithm	Bayesian Tables		Heuristics Tables	
	Highest Mean	Among Top	Highest Mean	Among Top
Random	-	-	0	0
Confidence	-	-	7	14
GLISTER	-	-	2	5
BALD	1	8	-	-
PowerBALD	0	2	-	-
SoftmaxBALD	0	1	-	-
SoftRankBALD	0	7	-	-
EPIG	1	15	-	-
PowerEPIG	0	2	-	-
SoftmaxEPIG	0	4	-	-
SoftRankEPIG	0	12	-	-
ParBaLS-MAP EPIG	8	20	6	16
ParBaLS EPIG	14	24	10	20

Table 7: Leaderboard summarizing the number of times each algorithm achieved the highest mean performance (Highest Mean) or was within the error bars of the best performing algorithm or vice versa (Among Top) across all 12 datasets and two budget settings.

the simpler one-vs-all settings, it is not as effective as ParBaLS in harder scenarios like tabular, text, or subpopulation-shifted datasets, as it fails to capture the irreducible uncertainty in tabular or text features and subpopulation shifts, which is not explored in previous studies.

We summarize the overall performance of the different algorithms in Table 7, where our ParBaLS EPIG outperforms all other algorithms, being within the top for 24 out of the 24 settings among the Bayesian-based AL algorithms and 20 out of the 24 settings when compared with state-of-the-art heuristics-based AL algorithms.

For visual illustration, we highlight the learning curves of the main algorithms on tabular datasets in Figure 4.

5 Related Work

5.1 Active Learning

Active Learning (AL) aims to reduce the cost of labeling training data by selecting the most informative data from a large unlabeled dataset that is infeasible to annotate it all [Settles, 2009]. Most previous lines of work focus on different heuristic criteria of the informativeness of the data, including but not limited to uncertainty (e.g., Confidence [Lewis, 1995], Margin [Scheffer et al., 2001], and Entropy [Wang and Shang, 2014]), diversity (e.g., CORESET [Sener and Savarese, 2018]), and a combination of both (e.g., BADGE [Ash et al., 2019], GALAXY [Zhang et al., 2022]). They are straightforward and easy to implement, but they lack a direct relationship to model performance, offering limited explanation for their good or bad performance. On the other hand, probabilistic methods [Houlsby et al., 2011, Gal et al., 2017, Kirsch et al., 2019, Ash et al., 2021, Kirsch et al., 2021, Killamsetty et al., 2021, Mussmann et al., 2022, Smith et al., 2023, Huseljic et al., 2024] are more statistically explainable, but their performance significantly varies due to unmet assumptions, such as the sufficiency of Top-B selection. Parallel to Rodemann et al. [2024] that unifies active learning, self-training, and multi-armed bandits algorithms into Reciprocal Learning, we aim to unify a more specific range of active learning algorithms into Myopic Bayesian Decision Theory and address its limitation in Batch Active Learning with ParBaLS.

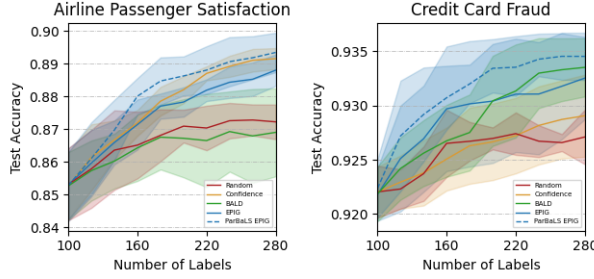


Figure 4: Test accuracy on tabular datasets with Bayesian Logistic Regression, where each of the 10 iterations has a labeling budget of 20 samples, except for the first iteration that starts with 100 samples.

5.2 Expected Error Reduction

Expected Error Reduction (EER) is one of the variants from the Myopic Bayesian Decision Theory (MBDT) that focuses directly on performance metrics like zero-one loss and log-likelihood loss [Kirsch et al., 2021, Mussmann et al., 2022, Smith et al., 2023], making them more interpretable and easier to understand potential issues with them. Some algorithms combine heuristic-based approaches with EER [Takahashi and Sato, 2024], making it more efficient than pure EER. However, it might lose some important samples that are not captured by heuristic algorithms. Some other algorithms explore a low-budget scenario to make EER more adaptive to real-world challenges [Zhao et al., 2024]. It employs an influence function to update models without retraining.

5.3 Pseudo-labeling in Active Learning

Unlike Unsupervised Learning or Semi-supervised Learning that aim to leverage more unlabeled data for training, Active Learning focuses on identifying and selecting fewer, but more informative data points to label. Some algorithms combine pseudo-labeling, a common semi-supervised learning technique, with active learning to handle the issue of a limited labeling budget from complementary directions [Tharwat and Schenck, 2023]. For example, Zhu et al. [2003] performs active learning on top of the pseudo-labeled samples, reducing the impact of the uneven quality of the pseudo labels. On the other hand, Gao et al. [2020] and Ji et al. [2025] combine several heuristic-based algorithms and use semi-supervision as the learner. Kirsch et al. [2021] and Rodemann et al. [2023] train a model with both real-labeled train data and pseudo-labeled evaluation data, which is used to compute acquisition scores for unlabeled data. In contrast, ParBaLS introduces a fundamentally different use of pseudo-labeling. Instead of contaminating the final labeled data with pseudo-labels, it only employs temporary pseudo-labels for constructing partial batches. This use of pseudo-labels is more similar to Jiang et al. [2017], which applies sequential simulation to facilitate batch active search, and Jiang et al. [2020], which aims to optimize a policy with nonmyopic Bayesian Optimization.

6 Conclusion

In this work, we derive a batched active learning algorithm from the Myopic Bayesian Decision Theory principle. While the algorithm is equivalent to EPIG [Kirsch et al., 2021, Smith et al., 2023] and EER [Roy and McCallum, 2001, Mussmann et al., 2022] for $B = 1$, it differs for larger batch sizes. In particular, to mitigate the batch acquisition issue of existing MBDT algorithms, we propose ParBaLS where we perform active learning with one-at-a-time queries but with sampled pseudo-labels. We show that ParBaLS EPIG outperforms other algorithms across several datasets and settings. We foresee a broad opportunity for future work to discover computationally efficient

approximations to scale the ParBaLS EPIG algorithm to larger datasets and models. In particular, incremental Bayesian learning methods could increase the computational efficiency. The effective algorithm derived from a general and intuitive principle empowers researchers and practitioners to better understand where an algorithm might go wrong, based on the modelling assumptions, and any approximations for computational efficiency.

One limitation is that simple heuristic-based algorithms like uncertainty sampling [Lewis, 1995] still outperforms principled probabilistic algorithms, including ParBaLS EPIG, in most of the one-vs-all image settings. As shown in Zhang et al. [2024] and Werner et al. [2024], uncertainty sampling works well on standard image datasets, but there are few studies about the reason behind the general observation. While ParBaLS remains a solid choice in a broad range of scenarios, we leave the study of why Confidence performs well and how ParBaLS can match its performance on benchmark image datasets settings for future work.

References

- Oriol Abril-Pla, Virgile Andreani, Colin Carroll, Larry Dong, Christopher J. Fonnesbeck, Maxim Kochurov, Ravin Kumar, Junpeng Lao, Christian C. Luhmann, O. A. Martin, Michael Osthege, Ricardo Vieira, Thomas V. Wiecki, and Robert Zinkov. Pymc: a modern, and comprehensive probabilistic programming framework in python. *PeerJ Computer Science*, 9, 2023. URL <https://api.semanticscholar.org/CorpusID:261469458>.
- Jordan Ash, Surbhi Goel, Akshay Krishnamurthy, and Sham Kakade. Gone fishing: Neural active learning with fisher embeddings. *Advances in Neural Information Processing Systems*, 34:8927–8939, 2021.
- Jordan T Ash, Chicheng Zhang, Akshay Krishnamurthy, John Langford, and Alekh Agarwal. Deep batch active learning by diverse, uncertain gradient lower bounds. In *International Conference on Learning Representations*, 2019.
- Sara Beery, Arushi Agarwal, Elijah Cole, and Vighnesh Birodkar. The iwildcam 2021 competition dataset. *arXiv preprint arXiv:2105.03494*, 2021.
- Gordon Christie, Neil Fendley, James Wilson, and Ryan Mukherjee. Functional map of the world. In *Proceedings of the IEEE Conference on Computer Vision and Pattern Recognition*, pages 6172–6180, 2018.
- Jacob Devlin, Ming-Wei Chang, Kenton Lee, and Kristina Toutanova. Bert: Pre-training of deep bidirectional transformers for language understanding. In *Proceedings of the 2019 conference of the North American chapter of the association for computational linguistics: human language technologies, volume 1 (long and short papers)*, pages 4171–4186, 2019.
- Yarin Gal, Riashat Islam, and Zoubin Ghahramani. Deep bayesian active learning with image data. In *International conference on machine learning*, pages 1183–1192. PMLR, 2017.
- Mingfei Gao, Zizhao Zhang, Guo Yu, Sercan Ö Arik, Larry S Davis, and Tomas Pfister. Consistency-based semi-supervised active learning: Towards minimizing labeling cost. In *European Conference on Computer Vision*, pages 510–526. Springer, 2020.
- Antonio Gulli. Ag’s corpus of news articles, 2004. URL http://groups.di.unipi.it/~gulli/AG_corpus_of_news_articles.html.
- Matthew D Hoffman, Andrew Gelman, et al. The no-u-turn sampler: adaptively setting path lengths in hamiltonian monte carlo. *J. Mach. Learn. Res.*, 15(1):1593–1623, 2014.
- Neil Houlsby, Ferenc Huszár, Zoubin Ghahramani, and Máté Lengyel. Bayesian active learning for classification and preference learning. *stat*, 1050:24, 2011.
- Denis Huseljic, Paul Hahn, Marek Herde, Lukas Rauch, and Bernhard Sick. Fast fishing: Approximating bait for efficient and scalable deep active image classification. In *Joint European Conference on Machine Learning and Knowledge Discovery in Databases*, pages 280–296. Springer, 2024.

- Xia Ji, LingZhu Wang, and XiaoHao Fang. Semi-supervised batch active learning based on mutual information. *Applied Intelligence*, 55(2):117, 2025.
- Shali Jiang, Gustavo Malkomes, Geoff Converse, Alyssa Shofner, Benjamin Moseley, and Roman Garnett. Efficient nonmyopic active search. In *International Conference on Machine Learning*, pages 1714–1723. PMLR, 2017.
- Shali Jiang, Daniel Jiang, Maximilian Balandat, Brian Karrer, Jacob Gardner, and Roman Garnett. Efficient nonmyopic bayesian optimization via one-shot multi-step trees. *Advances in Neural Information Processing Systems*, 33:18039–18049, 2020.
- Krishnateja Killamsetty, Durga Sivasubramanian, Ganesh Ramakrishnan, and Rishabh Iyer. Glister: Generalization based data subset selection for efficient and robust learning. In *Proceedings of the AAAI conference on artificial intelligence*, volume 35, pages 8110–8118, 2021.
- Andreas Kirsch, Joost Van Amersfoort, and Yarin Gal. Batchbald: Efficient and diverse batch acquisition for deep bayesian active learning. *Advances in neural information processing systems*, 32, 2019.
- Andreas Kirsch, Tom Rainforth, and Yarin Gal. Test distribution-aware active learning: A principled approach against distribution shift and outliers. *arXiv preprint arXiv:2106.11719*, 2021.
- Andreas Kirsch, Sebastian Farquhar, Parmida Atighehchian, Andrew Jesson, Frédéric Branchaud-Charron, and Yarin Gal. Stochastic batch acquisition: A simple baseline for deep active learning. *Transactions on Machine Learning Research*, 2023.
- TJ Klein. Airline passenger satisfaction. Kaggle, 2020. URL <https://www.kaggle.com/datasets/teejmahal20/airline-passenger-satisfaction>.
- Pang Wei Koh, Shiori Sagawa, Henrik Marklund, Sang Michael Xie, Marvin Zhang, Akshay Bal-subramani, Weihua Hu, Michihiro Yasunaga, Richard Lanas Phillips, Irena Gao, et al. Wilds: A benchmark of in-the-wild distribution shifts. In *International conference on machine learning*, pages 5637–5664. PMLR, 2021.
- Alex Krizhevsky, Geoffrey Hinton, et al. Learning multiple layers of features from tiny images. 2009.
- David D Lewis. A sequential algorithm for training text classifiers: Corrigendum and additional data. In *Acm Sigir Forum*, volume 29, pages 13–19. ACM New York, NY, USA, 1995.
- David J. C. MacKay. Information-based objective functions for active data selection. *Neural Computation*, 4(4):590–604, 07 1992. ISSN 0899-7667. doi: 10.1162/neco.1992.4.4.590. URL <https://doi.org/10.1162/neco.1992.4.4.590>.
- Stephen Mussmann, Julia Reisler, Daniel Tsai, Ehsan Mousavi, Shayne O’Brien, and Moises Goldszmidt. Active learning with expected error reduction. *arXiv preprint arXiv:2211.09283*, 2022.
- Dhanush Narayanan. Credit card fraud. Kaggle, 2022. URL <https://www.kaggle.com/datasets/dhanushnarayananr/credit-card-fraud>.
- Maxime Oquab, Timothée Darcet, Théo Moutakanni, Huy Vo, Marc Szafraniec, Vasil Khalidov, Pierre Fernandez, Daniel Haziza, Francisco Massa, Alaaeldin El-Nouby, et al. Dinov2: Learning robust visual features without supervision. *Transactions on Machine Learning Research Journal*, 2024.
- Gábor Pituk, Vik Shirvaikar, and Tom Rainforth. Do Bayesian neural networks actually behave like Bayesian models? In Aarti Singh, Maryam Fazel, Daniel Hsu, Simon Lacoste-Julien, Felix Berkenkamp, Tegan Maharaj, Kiri Wagstaff, and Jerry Zhu, editors, *Proceedings of the 42nd International Conference on Machine Learning*, volume 267 of *Proceedings of Machine Learning Research*, pages 49420–49458. PMLR, 13–19 Jul 2025. URL <https://proceedings.mlr.press/v267/pituk25a.html>.
- Alec Radford, Jong Wook Kim, Chris Hallacy, Aditya Ramesh, Gabriel Goh, Sandhini Agarwal, Girish Sastry, Amanda Askell, Pamela Mishkin, Jack Clark, et al. Learning transferable visual models from natural language supervision. In *International conference on machine learning*, pages 8748–8763. PMLR, 2021.

- Julian Rodemann, Jann Goschenhofer, Emilio Dorigatti, Thomas Nagler, and Thomas Augustin. Approximately bayes-optimal pseudo-label selection. In *Proceedings of the Thirty-Ninth Conference on Uncertainty in Artificial Intelligence*, UAI '23. JMLR.org, 2023.
- Julian Rodemann, Christoph Jansen, and Georg Schollmeyer. Reciprocal learning. *Advances in Neural Information Processing Systems*, 37:1686–1724, 2024.
- Nicholas Roy and Andrew McCallum. Toward optimal active learning through sampling estimation of error reduction. In *In Proc. 18th International Conf. on Machine Learning*, 2001.
- Tobias Scheffer, Christian Decomain, and Stefan Wrobel. Active hidden markov models for information extraction. In *International symposium on intelligent data analysis*, pages 309–318. Springer, 2001.
- Ozan Sener and Silvio Savarese. Active learning for convolutional neural networks: A core-set approach. In *International Conference on Learning Representations*, 2018.
- Burr Settles. Active learning literature survey. 2009.
- Freddie Bickford Smith, Andreas Kirsch, Sebastian Farquhar, Yarin Gal, Adam Foster, and Tom Rainforth. Prediction-oriented bayesian active learning. In *International conference on artificial intelligence and statistics*, pages 7331–7348. PMLR, 2023.
- Chako Takahashi and Toki Sato. Pool-based active classification based on expected error reduction with uncertainty subsampling. In *Asia Simulation Conference*, pages 244–255. Springer, 2024.
- Alaa Tharwat and Wolfram Schenck. A survey on active learning: State-of-the-art, practical challenges and research directions. *Mathematics*, 11(4):820, 2023.
- Dan Wang and Yi Shang. A new active labeling method for deep learning. In *2014 International joint conference on neural networks (IJCNN)*, pages 112–119. IEEE, 2014.
- Kai Wei, Rishabh K. Iyer, and Jeff A. Bilmes. Submodularity in data subset selection and active learning. In *International Conference on Machine Learning*, 2015. URL <https://api.semanticscholar.org/CorpusID:9176532>.
- Thorben Werner, Johannes Burchert, Maximilian Stubbemann, and Lars Schmidt-Thieme. A cross-domain benchmark for active learning. *Advances in Neural Information Processing Systems*, 37:62875–62911, 2024.
- Andy B. Yoo, Morris A. Jette, and Mark Grondona. Slurm: Simple linux utility for resource management. In Dror Feitelson, Larry Rudolph, and Uwe Schwiegelshohn, editors, *Job Scheduling Strategies for Parallel Processing*, pages 44–60, Berlin, Heidelberg, 2003. Springer Berlin Heidelberg. ISBN 978-3-540-39727-4.
- Jifan Zhang, Julian Katz-Samuels, and Robert Nowak. GALAXY: Graph-based active learning at the extreme. In Kamalika Chaudhuri, Stefanie Jegelka, Le Song, Csaba Szepesvari, Gang Niu, and Sivan Sabato, editors, *Proceedings of the 39th International Conference on Machine Learning*, volume 162 of *Proceedings of Machine Learning Research*, pages 26223–26238. PMLR, 17–23 Jul 2022. URL <https://proceedings.mlr.press/v162/zhang22k.html>.
- Jifan Zhang, Yifang Chen, Gregory Canal, Arnav Mohanty Das, Gantavya Bhatt, Stephen Mussmann, Yinglun Zhu, Jeff Bilmes, Simon Shaolei Du, Kevin Jamieson, et al. Labelbench: A comprehensive framework for benchmarking adaptive label-efficient learning. *Journal of Data-centric Machine Learning Research*, 2024.
- Zhuokai Zhao, Yibo Jiang, and Yuxin Chen. Direct acquisition optimization for low-budget active learning. In *NeurIPS 2024 Workshop on Bayesian Decision-making and Uncertainty*, 2024.
- Xiaojin Zhu, John Lafferty, and Zoubin Ghahramani. Combining active learning and semi-supervised learning using gaussian fields and harmonic functions. In *ICML 2003 workshop on the continuum from labeled to unlabeled data in machine learning and data mining*, volume 3, pages 58–65, 2003.

Algorithm 2 Active Learning

Input: active learning algorithm \mathcal{A} ;
 unlabeled pool dataset D ;
 unlabeled validation set V ;
 initial labeled data L_0 (e.g., randomly sampled);
 model training procedure M ;
 number of active learning iterations T ;
 budget for each iteration B

Output: Final model M_T and labeled set L_T

- 1: Train $M_0 = M(L_0)$
- 2: **for** iteration $t \leftarrow 1$ **to** T **do**
- 3: $S_t \leftarrow \mathcal{A}(D, V, L_{t-1}, M_{t-1}, B)$, where $S_t \subset D$ and $|S_t| = B$
- 4: $D \leftarrow D \setminus S_t$
- 5: Acquire labels for $x \in S_t$
- 6: $L_t \leftarrow L_{t-1} \cup \{(x, y) : x \in S_t\}$
- 7: Train $M_t = M(L_t)$
- 8: **end for**
- 9: **return** M_T and L_T

A Active Learning Formulation

As mentioned in Section 2.1, we outline the high-level structure of Active Learning in Algorithm 2.

B Theoretical Derivations

B.1 Notations

In the following derivations, we use upper-case letters for random variables, sets, and matrices, and lower-case letters for vectors and scalars.

Define Δ_S as the probability simplex over a finite set S . If S has n elements, $\Delta_S = \{p \in \mathbb{R}^n : p_i \geq 0, \sum_i p_i = 1\}$. Define Δ_S^k as the set of k -tuples of the probability simplex, $\Delta_S^k = \underbrace{\Delta_S \times \cdots \times \Delta_S}_{k \text{ times}}$

Define the entropy, conditional entropy, expected conditional entropy, and mutual information as,

$$H(X) = - \sum_x \Pr(X = x) \ln \Pr(X = x) \quad (7)$$

$$H(X|Z = z) = - \sum_x \Pr(X = x|Z = z) \ln \Pr(X = x|Z = z) \quad (8)$$

$$H(X|Z) = \sum_z \Pr(Z = z) H(X|Z = z) \quad (9)$$

$$I(X; Z) = H(X) - H(X|Z) \quad (10)$$

We use Y_x to refer to the random variable of the label of a point x . We take $y^{(i)}$ as an independent sample from $Y_D|L$.

B.2 Derivation of Optimal Predictions

As stated in Section 3, we can model myopic active learning as a two-step decision process, first choose a point to label, then choose predictions on the validation set. With this setup, the next point chosen to label is:

$$\arg \min_{\hat{x} \in D} \mathbb{E}_{\hat{y} \sim Y_{\hat{x}}|L} \left[\min_{P \in \Delta_{\mathcal{Y}}^{|V|}} \mathbb{E}_{\vec{y} \sim Y_V|Y_{\hat{x}} = \hat{y}, L} \left[\sum_{j=1}^{|V|} \ell(y_j, P_j) \right] \right] \quad (11)$$

We examine the second decision, the choice of validation predictions P ,

$$A(L, V, \hat{x}, \hat{y}) \stackrel{\text{def}}{=} \min_{P \in \Delta_{\mathcal{Y}}^{|V|}} \mathbb{E}_{\vec{y} \sim Y_V | Y_{\hat{x}} = \hat{y}, L} \left[\sum_{j=1}^{|V|} \ell(y_j, P_j) \right] \quad (12)$$

$$= \min_{P \in \Delta_{\mathcal{Y}}^{|V|}} \sum_{j=1}^{|V|} \mathbb{E}_{y_j \sim Y_{V_j} | Y_{\hat{x}} = \hat{y}, L} [\ell(y_j, P_j)] \quad (13)$$

$$= \sum_{j=1}^{|V|} \min_{p \in \Delta_{\mathcal{Y}}} \mathbb{E}_{y_j \sim Y_{V_j} | Y_{\hat{x}} = \hat{y}, L} [\ell(y_j, p)] \quad (14)$$

$$= \sum_{x \in V} \min_{p \in \Delta_{\mathcal{Y}}} \mathbb{E}_{y \sim Y_x | Y_{\hat{x}} = \hat{y}, L} [\ell(y, p)] \quad (15)$$

Using the negative log likelihood loss:

$$A(L, V, \hat{x}, \hat{y}) = \sum_{x \in V} \min_{p \in \Delta_{\mathcal{Y}}} \sum_{y \in \mathcal{Y}} \Pr(Y_x = y | Y_{\hat{x}} = \hat{y}, L) [-\ln p[y]] \quad (16)$$

Noting that the Hessian (with respect to p) is positive semi-definite, the function is convex in p . Using Lagrange multipliers (with the constraint $\sum_{y \in \mathcal{Y}} p[y] = 1$), we find that the optimal p has $p[y]$ proportional to (and thus equal to) $\Pr(Y_x = y | Y_{\hat{x}} = \hat{y}, L)$.

$$A(L, V, \hat{x}, \hat{y}) = \sum_{x \in V} \sum_{y \in \mathcal{Y}} \Pr(Y_x = y | Y_{\hat{x}} = \hat{y}, L) [-\ln \Pr(Y_x = y | Y_{\hat{x}} = \hat{y}, L)] \quad (17)$$

$$= \sum_{x \in V} H(Y_x | Y_{\hat{x}} = \hat{y}, L) \quad (18)$$

Thus, the next point is

$$\arg \min_{\hat{x} \in D} \mathbb{E}_{\hat{y} \sim Y_{\hat{x}} | L} \left[\min_{P \in \Delta_{\mathcal{Y}}^{|V|}} \mathbb{E}_{\vec{y} \sim Y_V | Y_{\hat{x}} = \hat{y}, L} \left[\sum_{j=1}^{|V|} \ell(y_j, P_j) \right] \right] \quad (19)$$

$$= \arg \min_{\hat{x} \in D} \mathbb{E}_{\hat{y} \sim Y_{\hat{x}} | L} \left[\sum_{x \in V} H(Y_x | Y_{\hat{x}} = \hat{y}, L) \right] \quad (20)$$

$$= \arg \min_{\hat{x} \in D} \sum_{x \in V} H(Y_x | Y_{\hat{x}}, L) \quad (21)$$

$$= \arg \min_{\hat{x} \in D} \sum_{x \in V} H(Y_x | L) - I(Y_x; Y_{\hat{x}} | L) \quad (22)$$

$$= \arg \max_{\hat{x} \in D} \sum_{x \in V} I(Y_x; Y_{\hat{x}} | L) \quad (23)$$

B.3 ParBaLS Monte Carlo Approximation Error

Here we show the approximation error from the Monte Carlo approximation is $\mathcal{O}(1/\sqrt{m})$ using a standard argument with a union bound and Hoeffding's inequality. With a partial batch of unlabeled samples S , using a similar derivation as above, the next point is:

$$\arg \max_{\hat{x} \in D} \mathbb{E}_{y_S \sim Y_S | L} \left[\sum_{x \in V} I(Y_x; Y_{\hat{x}} | Y_S = y_S, L) \right] \quad (24)$$

Define $f(\hat{x}, y_S) = \frac{1}{|V|} \sum_{x \in V} I(Y_x; Y_{\hat{x}} | Y_S = y_S^{(i)}, L)$ as a function of just y_S and \hat{x} with fixed S, L , and V . Thus, the next point chosen is,

$$\arg \max_{\hat{x} \in D} \mathbb{E}_{y_S \sim Y_S | L} [f(\hat{x}, y_S)] \quad (25)$$

Define the optimal ParBaLS point as x^* and the selected point using the Monte Carlo approximation as x_{MC} ,

$$x^* = \arg \max_{\hat{x} \in D} \mathbb{E}_{y_S \sim Y_S | L} \left[\sum_{x \in V} I(Y_x; Y_{\hat{x}} | Y_S = y_S, L) \right] = \arg \max_{\hat{x} \in D} \mathbb{E}_{y_S \sim Y_S | L} [f(\hat{x}, y_S)] \quad (26)$$

$$x_{\text{MC}} = \arg \max_{\hat{x} \in D} \frac{1}{m} \sum_{i=1}^m \sum_{x \in V} I(Y_x; Y_{\hat{x}} | Y_S = y_S^{(i)}, L) = \arg \max_{\hat{x} \in D} \frac{1}{m} \sum_{i=1}^m f(\hat{x}, y_S^{(i)}) \quad (27)$$

Noting that mutual information is positive and bounded by $\ln(|\mathcal{Y}|)$, $0 \leq f(x, y_S) \leq \ln(|\mathcal{Y}|)$. From Hoeffding's inequality, for a fixed $x \neq x^*$ and any $\epsilon > 0$,

$$\Pr \left(\frac{1}{m} \sum_{i=1}^m f(x, y_S^{(i)}) - \mathbb{E}_{y_S \sim Y_S | L} [f(x, y_S)] \geq \epsilon \right) \leq \exp \left(-\frac{2m\epsilon^2}{\ln^2(|\mathcal{Y}|)} \right) \quad (28)$$

Also,

$$\Pr \left(\frac{1}{m} \sum_{i=1}^m f(x^*, y_S^{(i)}) - \mathbb{E}_{y_S \sim Y_S | L} [f(x^*, y_S)] \leq -\epsilon \right) \leq \exp \left(-\frac{2m\epsilon^2}{\ln^2(|\mathcal{Y}|)} \right) \quad (29)$$

Union bounding over all elements of D , we have that with probability $|D| \exp \left(-\frac{2m\epsilon^2}{\ln^2(|\mathcal{Y}|)} \right)$,

$$\forall x \neq x^* : \frac{1}{m} \sum_{i=1}^m f(x, y_S^{(i)}) - \mathbb{E}_{y_S \sim Y_S | L} [f(x, y_S)] \leq \epsilon \quad (30)$$

$$\frac{1}{m} \sum_{i=1}^m f(x^*, y_S^{(i)}) - \mathbb{E}_{y_S \sim Y_S | L} [f(x^*, y_S)] \geq -\epsilon \quad (31)$$

Under such an event,

$$\mathbb{E}_{y_S \sim Y_S | L} [f(x^*, y_S)] - \mathbb{E}_{y_S \sim Y_S | L} [f(x_{\text{MC}}, y_S)] = \quad (32)$$

$$= \left[\mathbb{E}_{y_S \sim Y_S | L} [f(x^*, y_S)] - \frac{1}{m} \sum_{i=1}^m f(x^*, y_S^{(i)}) \right] + \quad (33)$$

$$+ \left[\frac{1}{m} \sum_{i=1}^m f(x^*, y_S^{(i)}) - \frac{1}{m} \sum_{i=1}^m f(x_{\text{MC}}, y_S^{(i)}) \right] + \quad (34)$$

$$+ \left[\frac{1}{m} \sum_{i=1}^m f(x_{\text{MC}}, y_S^{(i)}) - \mathbb{E}_{y_S \sim Y_S | L} [f(x_{\text{MC}}, y_S)] \right] \quad (35)$$

$$\leq \epsilon + 0 + \epsilon \quad (36)$$

$$= 2\epsilon \quad (37)$$

Solving for failure probability $\delta > 0$, with probability $1 - \delta$, the optimization gap is bounded by,

$$\mathbb{E}_{y_S \sim Y_S | L} [f(x^*, y_S)] - \mathbb{E}_{y_S \sim Y_S | L} [f(x_{\text{MC}}, y_S)] \leq 2 \ln(|\mathcal{Y}|) \sqrt{\frac{\ln(|D|) + \ln(1/\delta)}{2m}} \quad (38)$$

Thus, the optimization error introduced by the Monte Carlo approximation is $\mathcal{O}(1/\sqrt{m})$.

C Additional Experimental Results

C.1 Ablation Studies on Various Values of m and k , and Encoders with Small Budgets

In this section, we highlight results that also appear in our main experiments with [blue fonts](#).

Datasets Algorithm	Airline Passenger Satisfaction	Credit Card Fraud	One-vs-all				Subpopulation-shifted			
			CIFAR-10	CIFAR-100	iWildCam	fMoW	CIFAR-10	CIFAR-100	iWildCam	fMoW
ParBaLS-MAP EPIG	89.34±0.46	93.45±0.29	93.40±1.19	95.82±0.98	87.60±1.62	97.24±1.10	94.74±1.04	89.00±1.90	84.05±3.31	27.40±7.68
ParBaLS EPIG ($m = 5$)	89.45±0.58	93.37±0.13	93.80±1.18	96.20±0.72	85.52±0.64	97.93±0.64	94.72±0.77	88.40±3.07	80.45±5.15	38.63±8.33
ParBaLS EPIG ($m = 10$)	89.35±0.60	93.45±0.22	94.90±0.54	96.03±0.67	85.97±1.32	98.03±0.58	95.30±0.30	88.00±3.29	82.12±3.19	27.95±12.03
ParBaLS EPIG ($m = 20$)	89.70±0.55	93.49±0.20	94.17±0.72	96.66±0.87	85.80±1.60	98.30±0.72	95.26±0.59	88.60±3.07	80.97±3.11	32.05±12.78

Table 8: Final test accuracy of different variants of ParBaLS with Bayesian Logistic Regression, where each of the 10 iterations has a labeling budget of 20 samples, except for the first iteration that starts with 100 samples.

With $k = 400$ for the smaller budget settings, along with ParBaLS-MAP EPIG, we provide additional experimental results using three different numbers of universes for ParBaLS EPIG ($m = 5, 10, 20$) in Table 8, where $m = 10$ is the default setting in the main paper.

We notice that for each setting, all algorithms fall within the error bars of each other. While it appears that ParBaLS-MAP EPIG is as effective as the most expensive ParBaLS EPIG ($m = 20$) and is better than our default ParBaLS EPIG ($m = 10$), it overall underperforms ParBaLS EPIG ($m = 10$) in all other tables. This is because the occurrences of the highest mean for ParBaLS EPIG ($m = 10$) are reduced by the results of other m s in Table 8. Without them, ParBaLS EPIG ($m = 10$) has more occurrences of the highest mean than ParBaLS-MAP EPIG.

For different m s, we note that ParBaLS EPIG ($m = 5$) is the least effective one. While ParBaLS EPIG ($m = 20$) performs the best, its computational complexity is twice as much as ParBaLS EPIG ($m = 10$). In practice, ParBaLS EPIG ($m = 10$) is the most solid choice, given its balance between performance and complexity.

Next, we provide the ablation studies with $k = 200, 400, 800$ for the same budget in Table 9.

Datasets Algorithm	Airline Passenger Satisfaction	Credit Card Fraud	One-vs-all				Subpopulation-shifted			
			CIFAR-10	CIFAR-100	iWildCam	fMoW	CIFAR-10	CIFAR-100	iWildCam	fMoW
$k = 200$										
Random Confidence	87.33±0.59	92.71±0.23	87.26±0.76	88.44±0.78	83.43±1.18	90.45±1.32	76.00±4.20	65.80±9.79	74.02±4.31	17.95±7.38
BALD	89.20±0.63	92.73±0.47	95.28±0.63	98.36±0.49	90.49±1.70	99.09±0.38	82.30±2.03	44.40±9.09	79.23±4.36	6.58±4.76
PIIG	87.85±1.02	93.40±0.27	88.48±1.36	96.14±0.55	77.94±1.92	90.73±4.15	74.20±3.02	43.80±13.01	72.31±2.57	18.36±8.66
ParBaLS-MAP EPIG	88.74±0.31	93.27±0.36	91.23±1.06	93.48±1.19	84.62±3.03	95.81±0.60	90.92±0.66	88.20±3.19	81.06±2.10	18.49±9.17
ParBaLS EPIG	88.97±0.41	93.35±0.21	92.30±1.09	94.70±0.75	86.39±1.63	96.19±1.91	91.62±1.34	88.60±4.96	82.31±3.05	21.78±4.81
	89.14±0.54	93.54±0.10	93.80±0.86	97.13±0.46	88.31±1.62	97.28±1.32	93.32±0.74	89.00±3.29	82.51±2.09	31.51±11.07
$k = 400$										
Random Confidence	87.23±0.53	92.71±0.25	87.41±0.74	88.76±0.70	83.51±1.50	90.56±1.24	76.14±4.16	66.40±10.80	74.18±4.40	17.12±7.00
BALD	89.16±0.32	92.91±0.38	95.28±0.80	98.55±0.26	90.98±1.42	99.26±0.36	82.80±2.01	36.40±21.34	79.43±4.33	10.27±8.23
PIIG	86.91±1.35	93.35±0.27	87.21±1.39	95.28±1.06	74.95±1.51	89.82±3.31	72.98±1.89	37.80±16.33	70.87±1.96	23.56±3.67
ParBaLS-MAP EPIG	88.81±0.48	93.25±0.38	92.26±1.02	94.54±0.88	82.32±1.53	96.02±1.66	93.74±0.74	88.20±2.04	78.95±4.57	38.36±2.08
ParBaLS EPIG	89.34±0.46	93.45±0.29	93.40±1.19	95.82±0.98	87.60±1.62	97.24±1.10	94.74±1.04	89.00±1.90	84.05±3.31	27.40±7.68
	89.35±0.60	93.45±0.22	94.90±0.54	96.03±0.67	85.97±1.32	98.03±0.58	95.30±0.30	88.00±3.29	82.12±3.19	27.95±12.03
$k = 800$										
Random Confidence	87.25±0.56	92.72±0.22	87.44±0.45	88.74±0.67	83.58±1.41	90.71±1.12	76.30±4.24	65.20±10.61	74.11±4.61	17.12±6.47
BALD	89.52±0.30	92.91±0.34	94.77±1.38	98.68±0.36	89.38±1.19	99.27±0.54	79.88±0.50	41.80±18.73	79.33±4.54	9.45±4.23
PIIG	86.36±1.12	93.26±0.33	84.71±1.65	94.81±0.72	74.64±3.10	88.00±3.81	73.84±4.40	34.60±18.97	70.82±4.67	22.19±8.19
ParBaLS-MAP EPIG	89.08±0.47	93.41±0.15	92.08±1.42	92.71±1.17	80.76±3.41	96.88±0.75	95.80±0.84	88.00±4.47	76.09±4.92	33.70±4.49
ParBaLS EPIG	89.00±0.67	93.39±0.19	94.13±0.57	95.56±0.41	86.46±1.77	97.58±1.08	95.96±0.44	90.00±2.68	83.30±2.79	33.84±7.05
	89.36±0.21	93.24±0.26	93.92±0.75	96.09±0.99	87.18±1.36	98.22±0.21	96.50±0.46	88.20±1.60	82.35±3.80	32.88±7.09

Table 9: Final test accuracy with Bayesian Logistic Regression and $k = 200, 400, 800$, where each of the 10 iterations has a labeling budget of 20 samples, except for the first iteration that starts with 100 samples.

Last but not least, we show the ablation studies with the different encoders (see the original ones in Table 2) with $k = 400$ for the same budget in Table 10.

From the results, we observe that there is no significant difference in patterns for different k s or encoders, showing the consistency of our evaluation.

C.2 Learning Curves for Low Budget Settings on Image Datasets

Apart from the learning curves for the low budget settings of the tabular datasets in Figure 4, we also present the same settings for image datasets in Figure 5 for the one-vs-all setting and Figure 6 for the subpopulation-shifted setting.

Datasets Algorithm	One-vs-all				Subpopulation-shifted			
	CIFAR-10	CIFAR-100	iWildCam	fMoW	CIFAR-10	CIFAR-100	iWildCam	fMoW
CLIP-ViT-B/32								
Random	86.16 \pm 1.24	87.44 \pm 0.82	83.51 \pm 1.50	90.56 \pm 1.24	75.70 \pm 4.89	46.40 \pm 10.71	74.18 \pm 4.40	17.12 \pm 7.00
Confidence	94.25\pm0.40	96.17\pm0.61	90.98\pm1.42	99.26\pm0.36	82.44 \pm 2.71	38.00 \pm 8.67	79.43 \pm 4.33	10.27 \pm 8.23
BALD	81.47 \pm 1.12	89.10 \pm 2.01	74.95 \pm 1.51	89.82 \pm 3.31	80.14 \pm 3.18	29.60 \pm 10.98	70.87 \pm 1.96	23.56 \pm 3.67
EPIG	90.70 \pm 0.85	92.74 \pm 0.61	82.32 \pm 1.53	96.02 \pm 1.66	93.72 \pm 1.01	80.00\pm5.02	78.95 \pm 4.57	38.36\pm2.08
ParBaLS-MAP EPIG	91.46 \pm 0.77	94.08 \pm 0.19	87.60 \pm 1.62	97.24 \pm 1.10	93.58 \pm 0.94	82.60\pm4.18	84.05\pm3.31	27.40 \pm 7.68
ParBaLS EPIG	92.38 \pm 0.96	94.62 \pm 0.34	85.97 \pm 1.32	98.03 \pm 0.58	95.02\pm1.05	80.80\pm3.49	82.12\pm3.19	27.95\pm12.03
DINOv2-ViT-S/14								
Random	87.41\pm0.74	88.76\pm0.70	81.10 \pm 1.23	91.85 \pm 0.78	76.14\pm4.16	66.40\pm10.80	77.31 \pm 3.16	14.79 \pm 4.58
Confidence	95.28\pm0.80	98.55\pm0.26	86.53\pm1.06	99.74\pm0.06	82.80 \pm 2.01	36.40 \pm 21.34	77.72 \pm 3.69	4.79 \pm 7.59
BALD	87.21 \pm 1.39	95.28 \pm 1.06	76.01 \pm 2.08	95.91 \pm 0.70	72.98 \pm 1.89	37.80 \pm 16.33	68.25 \pm 2.04	5.89 \pm 1.76
EPIG	92.26 \pm 1.02	94.54 \pm 0.88	78.49 \pm 1.67	97.84 \pm 0.44	93.74 \pm 0.74	88.20\pm2.04	84.15\pm3.12	16.99 \pm 4.40
ParBaLS-MAP EPIG	93.40 \pm 1.19	95.82 \pm 0.98	79.23 \pm 1.63	86.35 \pm 1.00	94.74\pm1.04	89.00\pm1.90	81.97\pm1.17	25.21\pm7.16
ParBaLS EPIG	94.90\pm0.54	96.03 \pm 0.67	83.44 \pm 1.72	94.04 \pm 0.83	95.30\pm0.30	88.00\pm3.29	79.96 \pm 3.45	19.18\pm6.26

Table 10: Final test accuracy with Bayesian Logistic Regression ($k = 400$) and different encoders, where each of the 10 iterations has a labeling budget of 20 samples, except for the first iteration that starts with 100 samples.

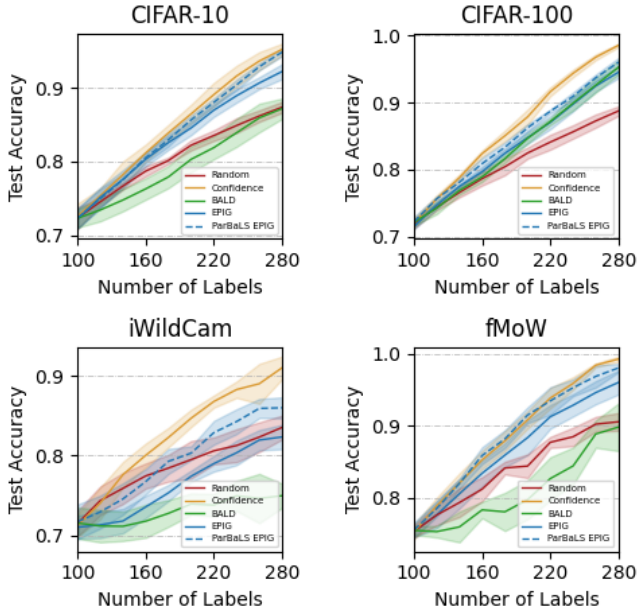


Figure 5: Test accuracy on one-vs-all image datasets with fixed encoders and trainable Bayesian Logistic Regression layer, where each of the 10 iterations has a labeling budget of 20 samples, except for the first iteration that starts with 100 samples.

C.3 Small Batch Acquisition versus Single Selection on Tabular Datasets

Considering the optimal myopic feature that EER objectives are designed for single selection, we conduct $T = 100$ iterations with each iteration budget of $B = 1$, as shown in Figure 7. However, single selection can be very inefficient in modern machine learning applications, as it requires a large number of data collection iterations. For example, with human annotation, hundreds of single selection iterations are difficult to crowd-source. Therefore, our ParBaLS for batch acquisition is more practical than single selection in many cases.

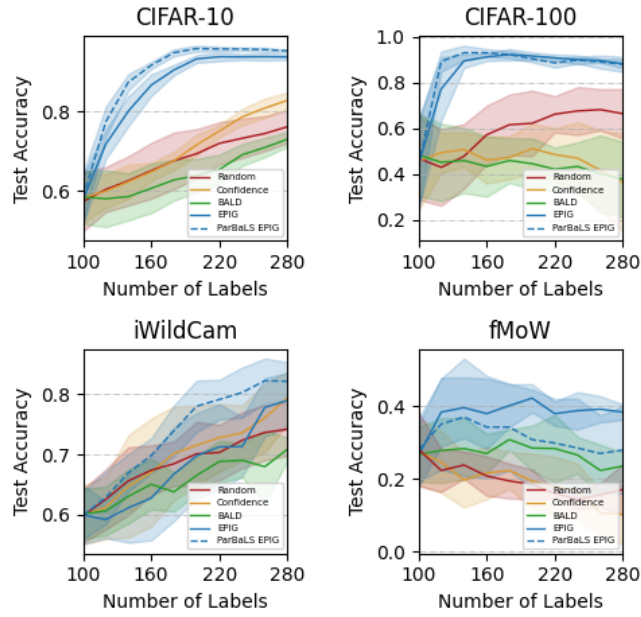


Figure 6: Test accuracy on subpopulation-shifted image datasets with fixed encoders and trainable Bayesian Logistic Regression layer, where each of the 10 iterations has a labeling budget of 20 samples, except for the first iteration that starts with 100 samples.

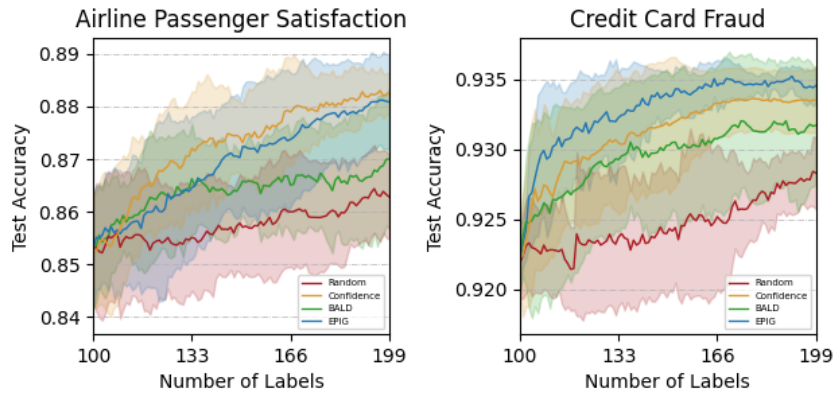


Figure 7: Test accuracy on tabular datasets with Bayesian Logistic Regression, where each of the 100 iterations has a labeling budget of 1 sample, except for the first iteration that starts with 100 samples.